JOURNAL OF MATERIALS SCIENCE **37** (2002) 3821 – 3826

Nanoindentation testing of plasma-polymerised hexane films

B. D. BEAKE*, S. ZHENG
Micro Materials Ltd., Unit 3, The Byre, Wrexham Technology Park, Wrexham, LL13 7YP, UK
E-mail: ben@micromaterials.co.uk

M. R. ALEXANDER
Corrosion and Protection Centre, UMIST, Manchester PO Box 88, M60 1QD, UK

The mechanical properties of plasma-polymerised hexane films have been investigated by nanoindentation. All the samples studied were harder and stiffer than conventional thermoplastic polymers and also exhibited lower creep rates. Systematic changes in the hardness and modulus were identified with varying deposition power, a parameter related to the degree of cross linking.

1. Introduction

Application of plasma polymers and inorganic plasma deposits, also obtained from organic precursors, has been realised in a diverse range of manufacturing sectors where well-adhered and pinhole-free thin coatings are desirable. Examples include corrosion protective barrier coatings on reflectors [1], gas permeation barrier coatings in packaging [2], coupling and coorrosion prevention layers on to steel [3], anti scratch and antireflective coating on polymeric ophthalmic lenses [4] and adhesion promotion pre-treatments on aluminium [5]. Film thicknesses of less than 100 nm are desirable in many of these applications.

Clearly, detailed knowledge of the relationship between the deposition parameters and the resultant mechanical properties of the plasma polymer is necessary if coatings are to be optimised for specific applications. Methods for evaluating the mechanical properties of bulk polymers, such as tensile and hardness testing, are clearly not suited to the investigation of supported thin films. For example, in microhardness testing, the large applied loads and penetration depths necessary to image the resultant indent result in an indentation response dominated by the underlying substrate [6].

To optimise the mechanical properties of plasma polymers and other thin polymer films it is necessary to use depth-sensing indentation (nanoindentation) to measure these properties on the nanoscale. Although more commonly used to characterise the mechanical properties of hard coatings and surface-modified layers [7–13], nanoindentation has been employed to investigate the mechanical properties of polymeric materials. These studies have shown that, with careful choice of the experimental parameters, nanoindentation can provide reliable quantitative measures of the hardness and the elasticity (modulus) of thick polymer films and bulk polymers [14–19].

To date there has been very little published work on the mechanical properties of plasma polymers. Benítez and co-workers have investigated the mechanical properties of thin films of plasma polymerised hexamethyl disiloxane in a DC glow discharge plasma [20–22]. The thin films were deposited on polycarbonate (PC) substrates and found to improve the mechanical properties of the PC. The hardness was found to vary with the composition of the gas mixture, with higher values obtained for oxygen/monomer mixtures than for those from pure HMDSO. In an earlier study, Kettle and co-workers determined a clear correlation between the elastic modulus of the sample and the flow rate of oxygen into the plasma [23], with increases in modulus from 2.06 GPa in pure HMDSO plasma to a maximum of 5.47 GPa at high oxygen flow rates. Both these research groups interpreted the differences in behaviour in terms of a transition between an effectively organic "polymer-like" film for the pure monomer to a more inorganic "silica-like" film when the proportion of oxygen in the gas mixture is increased. Characterisation of the chemistry of the films of Kettle *et al*. using X-ray photoelectron spectroscopy support this interpretation [24].

Here, we assess the suitability of nanoindentation to the characterisation of plasma polymerised hexane (ppHex) films. The influence of the deposition power (P) on the mechanical properties of the ppHex films is determined and compared to those of some conventional polymers.

2. Experimental

2.1. Materials

A range of in-plasma and downstream plasma-polymerised hexane films were prepared on aluminium (99.999%), that had been electropolished to give a smooth and defined surface at a cell voltage of 20 V

*Author to whom all correspondance should be addressed.

in an 80% ethanol/20% perchloric acid mixture at temperatures less than 5°C for 240 s. After electropolishing, the specimens were rinsed thoroughly in ethanol before drying in a cool air stream. The details of the plasma deposition apparatus are presented elsewhere [25]. Deposits on the electropolished aluminium were made both in and downstream of the plasma area with the thickness estimated using a quartz crystal microbalance located in a position equivalent to that of the sample and assuming a plasma polymer density of 1000 kg/m^3. Hexane (Aldrich) monomer was degassed using a freeze-thaw cycle prior to use. All ppHex samples were produced at a hexane flow rate of 2.0×10^{-6} m^{3}min^{-1} at standard temperature and pressure, and a pre-ignition pressure of 33 Pa (Base Pressure = 1 Pa). As a consequence of slower deposition rates for the downstream samples, these films were thinner than their in-plasma analogues.

2.2. Nanoindentation

A NanoTest System manufactured by Micro Materials was used for the nanoindentation testing. Details of the specifications of the instrument are published elsewhere [6, 7]. The NanoTest is a pendulum-based depth-sensing system, with the sample mounted vertically and the load applied electromagnetically as shown schematically in Fig. 1. Current in the coil causes the pendulum to rotate on its frictionless pivot so that the diamond probe penetrates the film surface. Test probe displacement is measured with a parallel plate capacitor achieving sub-nm resolution.

A Berkovich (three-sided pyramidal) diamond indenter was used throughout. The area function for the diamond (used to determine the contact area for a given depth) was calibrated by indentations into fused silica from 0.5–200 mN. The measured depth is subsequently adjusted for the effect of instrument compliance in the software before analysis. Two approaches to study the variation in mechanical properties with indentation depth were employed. These were (i) single repeat indentations to 0.2, 0.3, 0.6, 1.2, 5.0 and 10.0 mN and (ii) 20-cycle load-partial-unload experiments. Typical experimental conditions for the single indentations were:- initial load 0.02–0.03 mN, loading rate = unloading rate = 0.03–0.64 mN s^{-1}, 30–60 s holding period at peak load. Indentations were load-controlled (constant velocity) to a set maximum load (or to a maximum depth of 150 nm in some experiments) and were repeated on different regions of the film surface to determine the mechanical homogeneity of the samples. The load-partial-unload experiments covered the depth range 50–1500 nm. The loading and unloading rate was 0.21 mN/s and the dwell time was 30 s. The target unloading proportion was 10% of the current maximum load for that cycle. The data were analysed with the Oliver and Pharr method [9] as described below.

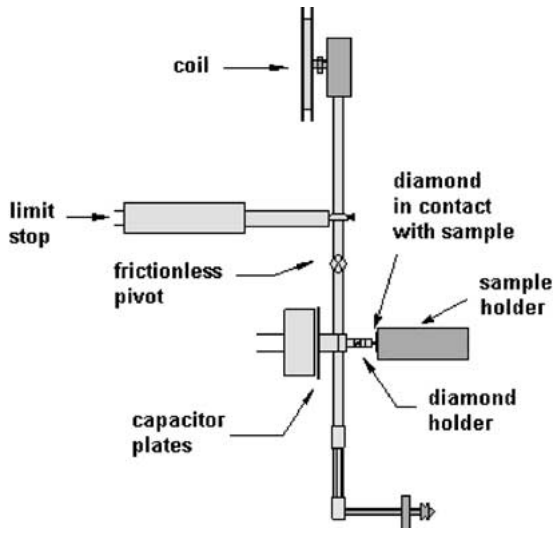

Figure 1 Schematic of the NanoTest system.

2.3. Indentation data analysis

A schematic of an idealised loading-unloading cycle from an elastoplastic material is shown in Fig. 2. For clarity creep occurring during the hold period at maximum load has been omitted. The depth vs. load unloading data was fitted to a power law function, as originally proposed by Oliver and Pharr [9], to determine the hardness and modulus of the film, after correction for the effects of instrument compliance (Equation 1).

$$\text{Contact compliance } (C) = \text{Total compliance } (C_t) - \text{Machine compliance } (C_m) \quad (1)$$

The power law function has the form

$$P = a(h - h_f)^m \quad (2)$$

where P is the load, $(h - h_f)$ is the elastic displacement, and a and m are material constants. The indenter contact (or plastic) depth, h_c, is determined from the expression:

$$h_c = h_{max} - \varepsilon(CP_{max}) \quad (3)$$

where C is the contact compliance equal to the tangent at maximum load (P_{max}). The value of ε depends on the pressure distribution that is established after the plastic deformation and is therefore a function of the indenter geometry. For flat punch indenter ε is 1, for a sphere ε is 0.75, cone ε is 0.72, and for a Berkovich indenter ε is taken as 0.75 since most indenters have a rounded tip. The plastic depths corresponding to these indenter geometries are shown in Fig. 2. The hardness (H) is determined from the peak load (P_{max}) and the projected

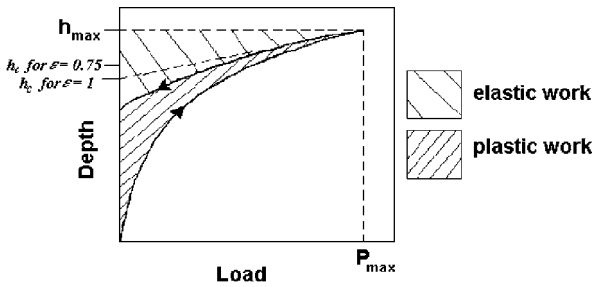

Figure 2 Schematic of the single indentation response from an idealised elasto-plastic material.

area of contact, A:

$$H = P_{\max}/A \tag{4}$$

The unloading portion of the depth-load curve is analysed according to Equation 5 to obtain the elastic modulus.

$$C = \pi^{0.5}/\left(2E_{\mathrm{r}}A^{0.5}\right) \tag{5}$$

where C is the contact compliance, A is the contact area and E_{r} is the reduced modulus defined by

$$1/E_{\mathrm{r}} = \left(1-\nu_{\mathrm{s}}^2\right)/E_{\mathrm{s}} + \left(1-\nu_{\mathrm{i}}^2\right)/E_{\mathrm{i}} \tag{6}$$

where ν_{s} = Poisson's ratio for the sample, ν_{i} = Poisson's ratio for the diamond indenter (0.07), E_{s} = Young's modulus for the sample and E_{i} = Young's modulus for the indenter (1141 GPa). In this paper E_{r} values are reported.

The creep data acquired during the holding period at maximum load (dwell time) were fitted by the general logarithmic equation for nanoindentation creep (Equation 7).

$$h = A\ln(Bt+1) \tag{7}$$

where h = increase in depth at maximum load, t = time, and A and B are fitting parameters.

3. Results

The plasma-polymer mechanical properties were investigated using both the single indentation and the load-partial-unload techniques.

Illustrative single-indentation curves from 1500 nm thick in-plasma samples deposited at 25 and 100 W are presented in Fig. 3. The film deposited at 100 W is harder and more elastic recovery is observed during unloading than for the 25 W film. The harder film is also more resistant to creep deformation occurring during the hold period (30 seconds) at maximum load. Repeated single indentations at different locations on the surface reveal lateral homogeneity of the indentation behaviour of the samples.

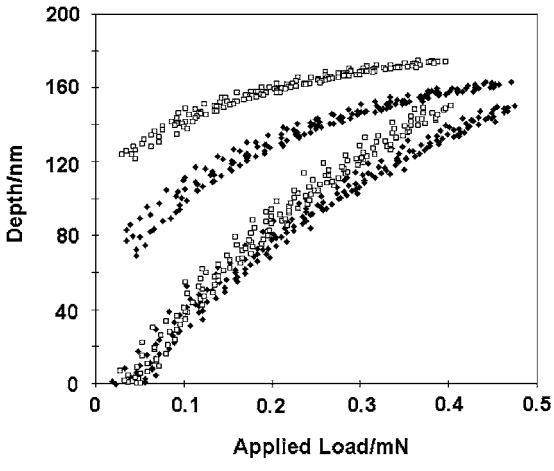

Figure 3 Typical single indentation measurements to maximum depth of 150 nm on a 1500 nm thick in-plasma films deposited at $P = 25$ W (open squares) and a 1500 nm thick $P = 100$ W (filled diamonds).

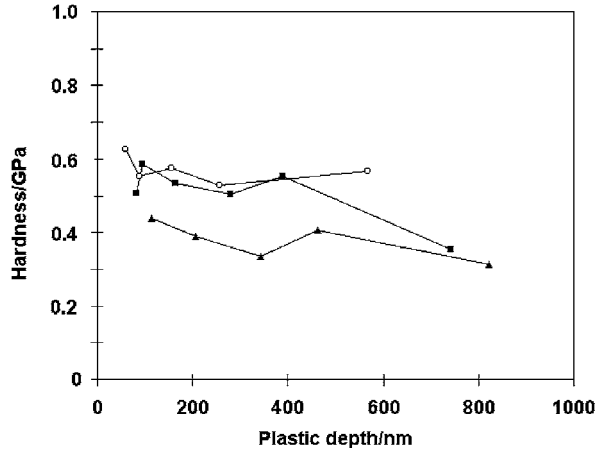

Figure 4 Variation in hardness with indentation depth for in-plasma films deposited at $P = 10$ W (triangles), $P = 25$ W (circles) and $P = 100$ W (squares) calculated from a number of single indents. The 25 W and 100 W films were 1500 nm thick and 10 W film was 300 nm thick.

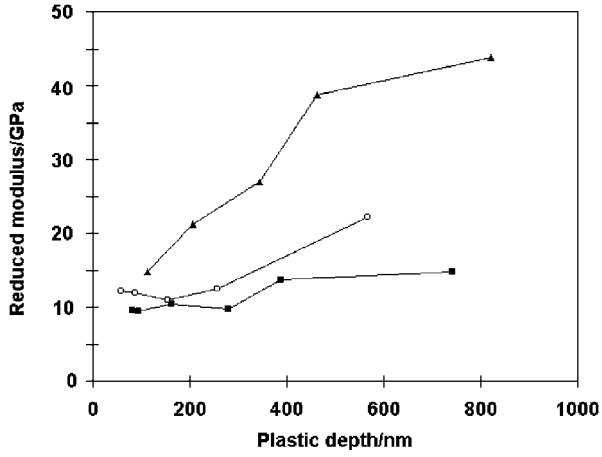

Figure 5 Variation in reduced modulus with indentation depth for in-plasma films deposited at $P = 10$ W (triangles), $P = 25$ W (circles) and $P = 100$ W (squares) calculated from a number of single indents. The 25 W and 100 W films were 1500 nm thick and 10 W film was 300 nm thick.

The variation in mechanical properties with indentation depth determined from repeated single indentations is shown for 100, 25 and 10 W films in Figs 4 and 5. Within the precision of the data, it is not possible show a clear trend in the hardness of the 25 or 100 W samples with depth at indentation depths less than 400 nm, although there may be a small increase in hardness approaching the surface of the coatings. The hardness of the 100 and 25 W films clearly decreases with increasing indentation depth after plastic depths of about 400 nm. The rapid increase in the modulus for the $P = 10$ W sample is indicative of the heightened influence of the aluminium substrate on this thinner (300 nm) coating.

The effect of loading rate and dwell time on the indentation behaviour are summarised in Table I. Varying the loading rate had little influence on the indentation behaviour of the 25 W films. The effect of varying the hold time on the mechanical properties of the plasma polymers is summarised in Tables II and III. Increasing the hold time from 30 to 180 s decreased the calculated hardness and slightly increased the elastic modulus.

TABLE I $P = 25$ W in-plasma films—variation in mechanical properties with hold time and loading rate

Deposition power (W)	Dwell time (s)	Load rate (mN/s)	Plastic depth (nm)	H (GPa)	E_r (GPa)
25	60	0.03	88	0.554 ± 0.031	11.96 ± 0.61
25	30	0.03	91	0.582 ± 0.033	12.27 ± 1.18
25	60	0.10	86	0.608 ± 0.038	12.51 ± 0.55

Repeat indentations to 0.3 mN. ppHex films were ~1500 nm thick. Standard errors in the mean quoted from ~5 repeat determinations.

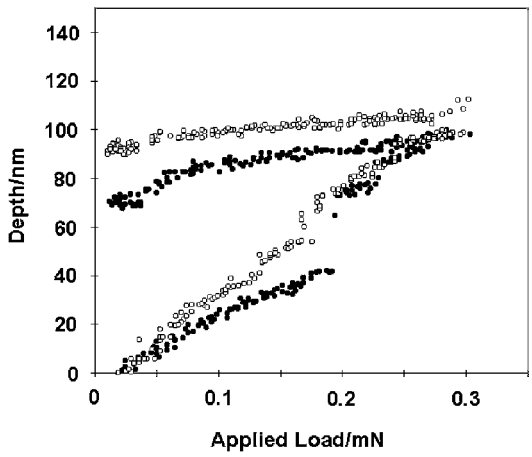

Figure 6 Typical single indentation measurement on 200 nm thick downstream films deposited at $P = 10$ W (open circles) and $P = 100$ W (filled circles).

Typical indentation behaviour for the samples deposited downstream of the plasma are presented in Fig. 6. In this figure clear discontinuities in displacement can be seen at critical loads of 0.19 and 0.24 mN on the 100 W sample and at 0.17 mN on the 10 W sample. Similar behaviour was seen in thinner (100 nm) in-plasma films deposited at 25 or 100 W.

In the load-partial-unload technique several loading-unloading cycles are performed at the same point to gradually increasing depth. The probe remains in contact throughout the test, unloading to a set proportion (10% of the maximum load for that cycle) before reloading to the next peak load. The technique gives a rapid overview of the variation in mechanical properties of the system as a function of depth.

The depth profile of the hardness and modulus determined using the partial unload technique is shown in Fig. 7. The hardness at shallow depths is similar to that derived from the single-indentations, such as those in Fig. 3. As the indentation depth was increased, the hardness of the film-substrate composite decreased and the modulus increased. The hardness (~0.30 GPa) and reduced modulus (~72 GPa) of the bare aluminium substrate were observed to be invariant with indentation depth.

TABLE III In-plasma films—analysis of creep data and comparison to other materials

Sample	Dwell period/s	Mean creep/nm	A	B
100 W ppHex	30	13.7 ± 1.0	3.79 ± 0.32	1.06 ± 0.12
25 W ppHex	30	22.6 ± 0.3	6.84 ± 0.09	0.81 ± 0.04
25 W ppHex	90	27.5 ± 0.5	6.62 ± 0.18	0.66 ± 0.05
25 W ppHex	180	30.4 ± 0.6	6.88 ± 0.19	0.40 ± 0.03
Uniaxially oriented PET*	60	77.0 ± 1.3	30.6*	0.19*
Uniaxially oriented PET‡	60	37	10.91‡	0.47‡
Fused silica	30	~8	2.22 ± 0.26	2.32 ± 0.43

All samples 1500 nm thick.
A and B are fitting parameters to the logarithmic creep equation $d = A \ln(Bt + 1)$.
PET = poly(ethylene terephthalate) film.
*5.0 mN indentations—data from Ref. 19.
‡0.5 mN indentation.

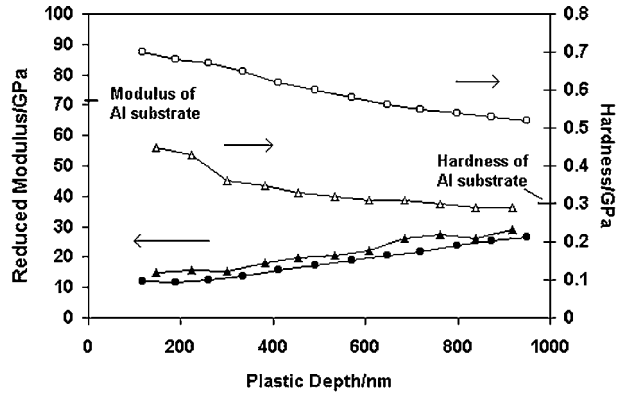

Figure 7 Depth profile of hardness and modulus from load-partial-unload experiments. Key:— for 1500 nm thick films deposited at $P = 100$ W—hardness (open circles) and reduced modulus (filled circles); for 1500 nm thick films deposited at $P = 25$ W—hardness (open triangles) and reduced modulus (filled triangles).

4. Discussion

4.1. Hardness and modulus: comparison with conventional thermoplastics

The in-plasma ppHex films studied in this work exhibited much greater hardness and stiffness than conventional (amorphous or crystalline) polymeric materials. For example, the reduced modulus of the

TABLE II In-plasma films—influence of hold time and deposition power on hardness and modulus

Power (W)	Dwell (s)	Max. depth (nm)	Plastic depth (nm)	Max. load (mN)	H (GPa)	E_r GPa
100	30	164 ± 2	130 ± 4	0.45 ± 0.02	0.679 ± 0.018	9.96 ± 0.16
25	30	175 ± 1	153 ± 1	0.41 ± 0.02	0.477 ± 0.009	13.47 ± 0.18
25	90	180 ± 1	161 ± 1	0.42 ± 0.02	0.444 ± 0.018	14.35 ± 0.26
25	180	185 ± 2	167 ± 2	0.42 ± 0.02	0.419 ± 0.008	15.10 ± 0.39

All samples were nominally 1500 nm thick.
10 repeat indentations at each point.

$P = 25$ W films (~14 GPa) is much larger than the reduced modulus of highly crystalline biaxially oriented poly(ethylene terephthalate) [PET] film determined by nanoindentation (~3 GPa) [19]. It is known that the deposition process produces a range from lightly to highly cross-linked materials depending on parameters relating to power input per monomer unit. The nanoindentation data show that this structure confers increased hardness to the films compared to a linear themoplastic polymer such as PET.

The behaviour of the plasma polymers shows much similarity to that of polymers which have been surface-modified by ion-irradiation techniques such as ion-implantation and plasma-enhanced ion implantation. These processes can lead to a highly cross-linked region at the surface of many polymers, which is hard, stiff and brittle [26–28]. Ion beam modifications have the potential to improve the tribological behaviour of polymers through shifting the dominant wear mechanism from abrasive or adhesive wear to slower fatigue wear processes [26]. The altered mechanical properties of the plasma polymerised coating will also influence the tribological performance of the material. We have previously shown that the deposition power has a dramatic influence on the nanotribology of the resultant film [29] and subsequently a critical load parameter has been developed to numerically express such data for comparison [30]. An AFM probe tip was used as a model single-asperity contact. The resistance to AFM tip-induced scratching wear increased with the deposition power. For the films deposited at higher powers, the resistance to scratching was much better than for conventional polymers such as PET.

Cross-linked polymers usually exhibit a much lower E/H ratio than unmodified polymers. For example, Dong and Bell have shown [26, 28] that although plasma immersion ion implantation of UHMWPE can lead to a seven-fold increase in hardness from 50 to 350 MPa, the elastic modulus is less than doubled (840 to 1453 MPa), causing the E/H ratio to decrease from 16.8 to 4.2. This change was accompanied by an improvement in the wear resistance of the modified polymer by a factor of 10. The data in Table II and Figs 4–6 show that the E/H ratio on ppHex films does decrease with higher deposition power, in line with the expected greater cross-link density, although it is necessary to compare with data on shallow indentations in view of the lower film thickness on the $P = 10$ W sample.

4.2. Variation in mechanical properties with indentation depth

The mechanical property data show fairly typical behaviour for a harder coating on a softer substrate. Similar trends were obtained using the load-partial-unload and the repeat single indentation techniques. When the indentation depth is a small proportion of the coating thickness, the stress field remains within the plasma polymerised film and the mechanical properties are essentially those of the coating without substrate influence. Fig. 4 shows that, within the experimental scatter, there is no clear variation in the measured hardness with depth within ~400 nm of the surface, the constant hardness (0.5–0.6 GPa) suggesting the structure of the ppHex films varies little with distance from the coating surface. Fig. 7 shows that at plastic depths greater than ~300–400 nm the influence of the underlying substrate on the (composite) indentation response increases with the indentation depth, as expected. Since the aluminium substrate is much stiffer than the plasma polymer film, this leads to a continuous rise in the elastic modulus with depth. The more rapid rise in modulus on the $P = 10$ W sample seen in Fig. 5 is due to the lower film thickness of this sample; the substrate influence is felt at considerably smaller indentation depths.

4.3. Creep deformation

Since hardness is derived from the contact depth at maximum load, it is affected by creep deformation occurring during the dwell time (holding period) at maximum load. It is known that that if this holding period is absent, the sample will continue to deform viscoplastically during unloading, distorting the shape of the unloading curve and leading to inaccurate values of the modulus, since it is determined from the tangent to the slope of the unloading curve at maximum load [15, 17, 19]. The data in Table II show that as the dwell time is increased the calculated hardness decreases slightly, whereas the elastic modulus increases slightly. In microhardness and depth-sensing testing of polymers, the time-dependent part of the plastic deformation (i.e. creep) generally follows a function of the type shown in Equation 8 [6, 17].

$$H = H_0 t^{-k} \tag{8}$$

where H_0 is the hardness measured at $t = 1$ min and k is the creep constant. An approximate value for k of 0.07 can be estimated from the data in Table II. This can be compared with k values of ~0.04 on PET and ~0.09 on poly(ethylene oxide) [PEO], although it should be noted that as these two materials are much softer than the plasma polymers, these k values correspond to a much greater % change in their hardness with hold time.

The slight increase in modulus with increasing dwell time was somewhat unexpected, although Flores and Baltá Calleja have observed a similar time-dependent behaviour on indenting amorphous PET films to a peak load of 150 mN and holding at maximum load for up to 10 min [17]. They interpreted this behaviour as greater viscoelastic recovery occurring during unloading with shorter holding times.

The creep data (depth increase vs. hold time) were found to follow the general logarithmic creep formula (Equation 8) which has recently been used to describe the nanoindentation creep behaviour of PET [19], PEO [31], glasses, ceramics and thin DLC coatings [32]. Typical creep data for PET and fused silica are shown in Table III for comparison. The parameter A is a measure of the general susceptibility to creep whilst the parameter B is a measure of the rate of the exponential creep process. Table III shows that increasing hold time had little effect on the parameter A but decreased B. The slight decrease in B with time suggests that the fit to the creep equation is not exact, and hence the actual creep

rate decreases more rapidly than predicted by the data from short dwell times. Time-dependent plastic deformation (e.g., polymer chains moving relative to each other) appears to be significantly restricted by the extensive cross-linking. The plasma polymers exhibit better creep resistance than conventional semicrystalline thermoplastics such as PEO or PET, and the $P = 100$ W sample approaches the creep resistance of fused silica.

4.4. Downstream samples

The samples deposited downstream of the plasma exhibited cracking during loading. In view of this cracking, hardness and modulus values determined on the downstream samples are less reliable than those on the in-plasma films. Similar cracking in thin (100 nm) in-plasma coatings points to the thinness of the coatings being the cause, although another possibility is poor adherence of the coating to the substrate.

5. Conclusions

The mechanical properties of plasma-polymerised hexane films have been investigated by nanoindentation. There were clear differences with the deposition power, a parameter related to the degree of cross-linking. The samples studied were harder and stiffer than conventional thermoplastic polymers. They also exhibited much lower creep rates, which approached those of fused silica. The work has shown the capability of nanoindentation to study these materials and has identified suggested a process parameter by which their mechanical properties can be tailored for given applications.

Acknowledgements

The authors would like to acknowledge Dr. S. R. Goodes (Micro Materials) for writing the software for the analysis of the creep data and for helpful discussions.

References

1. G. BENZ, *Bosch. Techn. Ber.* **8** (1997) 219.
2. M. CREATORE, F. PALUMBO, R. D'AGOSTINO and P. FAYET, *Surf. Coat. Tech.* **142** (2001) 163.
3. T. J. LIN, J. A. ANTONELLI, D. J. YANG, H. K. YASUDA and F. T. WANG, *Progress in Organic Coatings* **31** (1997) 351.
4. U. HAYAT, *J. Macromol. Sci.—Pure Appl. Chem.* A **31** (1994) 665.
5. M. R. ALEXANDER, X. ZHOU, G. E. THOMPSON, T. M. DUC, E. MCAPLINE and B. J. TIELSCH, *Surface and Interface Analysis* **30** (2000) 16.
6. F. J. BALTÁ CALLEJA and S. FAKIROV in "Microhardness of Polymers" (Cambridge University Press, Cambridge, UK, 2000).
7. H. M. POLLOCK, "Nanoindentation," ASM Handbook, Vol. 18 (1992) p. 419.
8. M. F. DOERNER and W. D. NIX, *J. Mat. Res.* **1** (1986) 601.
9. W. C. OLIVER and G. M. PHARR, *ibid.* **7** (1992) 1564.
10. E. MARTÍNEZ, M. C. POLO, E. PASCUAL and J. ESTEVE, *Diam. Relat. Mater.* **8** (1999) 563.
11. A. LOUSA, E. MARTÍNEZ, J. ESTEVE and E. PASCUAL, *Thin Solid Films* **355/356** (1999) 210.
12. J. ESTEVE, E. MARTÍNEZ, A. LOUSA, F. MONTALÁ and L. L. CARRERAS, *Surf. Coat. Tech.* **133/134** (2000) 314.
13. J. L. MENEVE, J. F. SMITH, N. M. JENNETT and S. R. SAUNDERS, *Appl. Surf. Sci.* **100/101** (1996) 64.
14. R. H. ION, H. M. POLLOCK and C. ROQUES-CARMES, *J. Mater. Sci.* **25** (1990) 1444.
15. B. J. BRISCOE, L. FIORI and E. PELILLO, *J. Phys.* D **31** (1998) 2395.
16. R. S. DWYER-JOYCE, Y. USHIJIMA, Y. MURAKAMI and R. SHIBUTA, *Tribol. Int.* **31** (1998) 525.
17. A. FLORES and F. J. BALTÁCALLEJA, *Phil. Mag.* A **78** (1998) 1283.
18. M. R. VANLANDINGHAM, J. S. VILLARRUBIA, W. F. GUTHRIE and G. F. MEYERS, *Macromol. Symp.* **167** (2001) 15.
19. B. D. BEAKE and G. J. LEGGETT, *Polymer* **43** (2002) 319.
20. F. BENÍTEZ, E. MARTÍNEZ, M. GALÁN, J. SERRAT and J. ESTEVE, *Surf. Coat. Tech.* **125** (2000) 383.
21. J. ESTEVE, F. BENÍTEZ, S. BOSCH, E. MARTÍNEZ, M. GALÁN and J. SERRAT, in Proc. SPIE 2000, San Diego.
22. F. BENÍTEZ, E. MARTÍNEZ and J. ESTEVE, *Thin Solid Films* **377/378** (2000) 109.
23. A. P. KETTLE, F. R. JONES, M. R. ALEXANDER, R. D. SHORT, M. STOLLENWERK, J. ZABOLD, W. MICHAELI, W. WU, E. JACOBS and I. VERPOEST, *Composites* A **29A** (1998) 241.
24. M. R. ALEXANDER, R. D. SHORT, F. R. JONES, W. MICHAELI and C. BLOMFIELD, *Applied Surface Science* **137** (1999) 179.
25. M. R. ALEXANDER and T. M. DUC, *J. Mat. Chem.* **8** (1998) 937.
26. H. DONG and T. BELL, *Surf. Coat. Tech.* **111** (1999) 29.
27. J. C. PIVIN, *Nucl. Instrum. Meth.* B **84** (1994) 484.
28. H. DONG and T. BELL *et al.*, First Annual Project Report, Inco-Copernicus IC15-CT96-0705 (1998).
29. B. D. BEAKE, G. J. LEGGETT and M. R. ALEXANDER, *Polymer* **42** (2001) 2647.
30. F. DINELLI, G. J. LEGGETT and M. R. ALEXANDER, *J. Appl. Phys.* **91** (2002) 3841.
31. B. D. BEAKE, S. CHEN, J. B. HULL and F. GAO, *J. Nanosci. Nanotech.* **2** (2002) 73.
32. T. CHUDOBA and F. RICHTER, *Surf. Coat. Tech.* **148** (2001) 191.

Received 22 January
and accepted 21 May 2002